Stabilization of Line Tied Resistive Wall Kink Modes with Rotating Walls

C. C. Hegna

Department of Engineering Physics

University of Wisconsin

Madison, WI 53706-1687

April 14, 2004

Abstract

A method suggested by Gimblett[(C. G. Gimblett, *Plasma Phys. Controlled Fusion* **31**, 2183 (1989)] for stabilizing resistive wall modes by using a rotating double wall configuration is applied to a line tied screw pinch equilibrium. The line tied boundary conditions provide an additional stabilizing mechanism relative to instabilities present in periodic cylinders. For a given equilibrium, there exist an optimal spacing between a stationary and a rotating wall which minimizes the critical wall rotation frequency for stabilization.

Pacs. nos. 52.35.Py, 52.55.DY, 52.30-q

I. INTRODUCTION

A novel method for passively stabilizing the resistive wall mode (RWM) was suggested by Gimblett [1]. In the Gimblett configuration, two resistive walls are used that rotate relative to one another. If both walls are inside the critical radius for wall stabilization of the external kink and the walls are separated radially, sufficiently large differential rotation of the walls is capable of stabilizing the RWM. In the following, we apply this idea to a line-tied screw pinch configuration.

A number of authors have addressed the effect of rotating walls on RWMs in periodic cylinder geometry [2, 3, 4, 5]. What distinguishes this work from prior investigations is the effect of line tied boundary conditions. This axial boundary condition provides a substantial stabilizing effect [6, 7]. Unlike the case of a periodic cylinder, where the linear response of magnetic perturbations can be represented by isolated Fourier harmonic $\tilde{\mathbf{B}} \sim e^{im\theta - n\zeta}$ (where θ and ζ are the poloidal and toroidal angles, respectively and m and n are integers), line tied boundary conditions require that the eigenmode satisfy a partial differential equation. Namely, the magnetic perturbation is written $\tilde{\mathbf{B}} = \tilde{\mathbf{B}}(r,z)e^{im\theta}$ and $\tilde{\mathbf{B}}$ is required to satisfy both radial and axial boundary conditions [$\tilde{B}_r(z=0) = \tilde{B}_r(z=L) = 0$ for a configuration with axial length L]. As has been shown by Ryutov and co-workers [8], the effect of conducting end walls makes analysis of the stability problem more complex. In this work, we account for line tied boundary conditions and the presence of two differentially rotating walls whose radii lie outside the plasma region;

the walls have radial locations $r = b, c$ with $a \leq b \leq c$ where $r = a$ is the plasma vacuum interface.

The ability to stabilize long wavelength external kink modes is a crucial issue for a number of toroidal confinement concepts. The tokamak, spherical tokamak (ST) and reversed field pinch (RFP) configurations rely on the existence of a perfectly conducting wall at the plasma boundary to stabilize external MHD modes. Stabilization of pressure driven kinks in advanced tokamaks allows one to exceed the obtainable $\beta(= 2\mu_o p/B^2)$ limits by a substantial fraction over the β limit of the no-wall configuration. This leverage is amplified in ST configurations where the presence of a perfectly conducting wall is predicted to increase the β limit by a factor of order unity. In an RFP, a number of external modes are predicted to be unstable which makes the presence of a conducting wall a necessity for stable operation.

While perfect conducting walls can provide robust stabilization to external ideal MHD modes, a finite amount of conductivity in the wall causes the stabilizing wall eddy currents to decay away. On the timescale of the wall, τ_w, flux can leak through the wall and provide a mechanism by which the plasma can access the free-energy available to the external kink. This mode, the resistive wall mode (RWM) grows on the τ_w timescale which is typically much longer than the growth rate of ideal external kink. In the absence of plasma flows [9], if the plasma is unstable without a wall, there will always be either an RWM or an external kink; the plasma is always unstable. The RWM has been identified in a number of devices [10, 11].

The advanced tokamak program is addressing means by which to stabilize the RWM by using active methods to control the plasma rotation [12], and by using feedback with magnetic coils [13, 14, 15]. The Gimblett double wall configuration does not require active means to suppress an instability. Rather, differentially rotating walls of sufficient amplitude allow access to operating regimes that would be unstable to RWMs if the walls were stationary. For a given MHD equilibrium that is unstable without a conducting wall, there exists a critical rotation rate for RWM stabilization provided both walls are inside the critial radius. A related RWM suppression technique that can be implemented in toroidal plasma is to use flowing liquid metal walls [16]. While there are some important differences, the double wall configuration also models flowing walls as well [4, 5]. Additionally, there are distinct similarities between the mathematics of describing the double wall configuration and the treatment of resistive wall tearing modes [17, 18]. Plasma rotation is known to have a stabilizing effect on resistive wall tearing modes.

Prompted by the interest in seeking methods to stabilize the resistive wall modes, a small experiment was proposed at the University of Wisconsin to address the viability of the Gimblett configuration [19]. The configuration to be used is a line-tied screw pinch. The initial experiments will use two resistive walls spaced radially from each other where the outer wall is allowed to rotate poloidally relative to an inner statitionary wall. The theory to follow is directly relevant to this configuration. The second set of experiments will use flowing liquid metal as a replacement for the rotating wall.

In the following section, we review the essential features of the stability properties of the configuration. In Section II.A, the magnetostatic equilibrium and structure of the linear perturbation in the screw pinch geometry is introduced. In section II.B, we specialize to the case of a constant current profile in the plasma region and derive an equation from which the linear eigenvalue can be calculated. In Sec. II.C, the roles of stationary and rotating resistive wall are described and a linear dispersion is derived in Sec.II.D for this configuration. Here, the specific role of differentially rotating walls is addressed and a prediction for the critical rotation rate for RWM stabilization is presented. In Section III, we briefly review the equivalent stability calculation for the periodic cylinder and compare this result to the line tied configuration. Finally, a discussion of the results in given in Section IV.

II. MODEL

The particular geometry to be studied is a cylinder of length L and with a plasma radius $r = a$. The plasma is described by the ideal magnetohydrodynamic (MHD) equations. For simplicity, we consider a force free equilibrium ($\nabla p_o = 0$) and a large aspect approximation $a \ll L$. The axial boundary conditions are set by the presence of conducting end walls at $z = 0$ and $z = L$. Radially, two thin shell resistive walls are present at $r = b$ and $r = c$ with $a \leq b \leq c$. The only dissipation accounted for in the problem is the finite resistivity of these walls.

A. Equilibrium and linear perturbation

A force free equilibrium is used and given by

$$\mathbf{B}_o = B_{z0}(r)\hat{\mathbf{z}} + B_{\theta 0}(r)\hat{\theta}, \tag{1}$$

$$\nabla \times \mathbf{B}_o = \frac{\lambda(r)}{\mu_o}\mathbf{B}_o. \tag{2}$$

In the following, a tokamak ordering ($B_{\theta 0} \ll B_{z0}$) is assumed. An effective "q" profile can be defined by

$$q(r) = \frac{2\pi r B_{z0}(r)}{L B_{\theta 0}}, \tag{3}$$

which is an order unity quantity in the large aspect ratio approximation. In this limit, the current profile is given by

$$\lambda(r) = \frac{1}{rB_{z0}}\frac{d}{dr}(rB_{\theta 0}) + \mathcal{O}(\frac{a}{L})^2. \tag{4}$$

Since symmetry exists in the poloidal direction, the linear mode can be Fourier analyzed ($\tilde{\xi} \sim e^{im\theta}$). For simplicity, $m = 1$ is treated in the following. The ideal MHD displacement vector and magnetic perturbation are written

$$\tilde{\xi} = \xi(r, z)e^{i\theta}, \tag{5}$$

$$\tilde{\mathbf{B}} = \mathbf{B}(r, z)e^{i\theta}. \tag{6}$$

The linear momentum and induction equations are

$$-\omega^2 \rho_o \tilde{\xi} = \tilde{\mathbf{J}} \times \mathbf{B}_o + \frac{\lambda}{\mu_o}\mathbf{B}_o \times \tilde{\mathbf{B}} - \nabla \tilde{p}, \tag{7}$$

$$\tilde{\mathbf{B}} = \nabla \times (\tilde{\xi} \times \mathbf{B}_o), \tag{8}$$

where $\mu_o\tilde{\mathbf{J}} = \nabla \times \tilde{\mathbf{B}}$ and the mass density ρ_o is constant in the plasma region. The perturbed pressure satisfies $\tilde{p} = -\gamma p_o \nabla \cdot \tilde{\xi}$ and plays no role for incompressible plasmas, $\tilde{p} = 0$. In this limit, the parallel component of the momentum balance equation becomes $\mathbf{B}_o \cdot \tilde{\xi} = 0$. Hence, the displacement vector can be written

$$\tilde{\xi} = \tilde{\xi}_r \hat{\mathbf{r}} + \tilde{\xi}_\perp \hat{\mathbf{b}}_o \times \hat{\mathbf{r}}, \tag{9}$$

where $\hat{\mathbf{b}}_o = \mathbf{B}_o/|\mathbf{B}_o|$. With an incompressibility approximation, $\nabla \cdot \tilde{\xi} = 0$, one finds

$$\frac{1}{r}\frac{\partial}{\partial r}(r\tilde{\xi}_r) + \nabla \cdot (\tilde{\xi}_\perp \hat{\mathbf{b}}_o \times \hat{\mathbf{r}}) = \frac{1}{r}\frac{\partial}{\partial r}(r\tilde{\xi}_r) + \frac{i}{r}\tilde{\xi}_\perp[1 + \mathcal{O}(\frac{a}{L})^2] = 0. \tag{10}$$

The incompressibility approximation is only strictly valid at marginal ideal MHD stability, and therefore valid in calculating the RWM dispersion relation when the wall time exceeds characteristic Alfven times. However, compressibility effects would alter the growth rate of the ideal MHD external kink.

Combining two components of the momentum equation, Eq. (7), and Eq. (10) yields the expression

$$\omega^2 \nabla_\perp \cdot [\mu_o \rho_o \nabla_\perp (r\tilde{\xi}_r)] = -\mathbf{B}_o \cdot \nabla[\nabla_\perp^2 (r\tilde{B}_r)] + \frac{iB_0}{r}\frac{d\lambda}{dr}(r\tilde{B}_r), \tag{11}$$

where

$$\nabla_\perp^2 = \frac{1}{r}\frac{\partial}{\partial r}(r\frac{\partial}{\partial r}) + \frac{1}{r^2}\frac{\partial^2}{\partial \theta^2}. \tag{12}$$

B. Constant current profile

For a specific calculation, the current profile is taken to be flat in the plasma region ($0 < r < a$),

$$\lambda(r) = \lambda_o \Theta(a - r), \tag{13}$$

where λ_o is a constant and $\Theta(x)$ is the Heaviside step function. For this current profile, the $q(r)$ profile is constant for $r < a$ [$q(r) = q_a = 4\pi/(\lambda_o L)$] and increases parabolically for $r > a$. With this equilibrium, a jump condition at the plasma vacuum interface can be derived from Eq. (11),

$$\omega^2 (a\mu_o \rho_o) \frac{d}{dr}(r\tilde{\xi}_r)|_{a-}^{a+} = -(\mathbf{B}_o \cdot \nabla) a \frac{d}{dr}(r\tilde{B}_r)|_{a-}^{a+} + iB_o a \tilde{B}_r \lambda|_{a-}^{a+}. \tag{14}$$

With $\rho = \lambda = 0$ for $r = a+$, this expression reduces to

$$\omega^2 \mu_o \rho_o \tilde{\xi}_a \Delta_\xi = (\mathbf{B}_0 \cdot \nabla)\tilde{B}_a(\Delta_+ - \Delta_-) + iB_0 \lambda_0 \tilde{B}_a, \tag{15}$$

where $\tilde{B}_a = \tilde{B}_r(r = a)$, $\tilde{\xi}_a = \tilde{\xi}_r(r = a)$, and

$$\Delta_\xi = \frac{1}{\tilde{\xi}_a} \frac{d}{dr}(r\tilde{\xi})|_{r=a-}, \tag{16}$$

$$\Delta_- = \frac{1}{\tilde{B}_a} \frac{d}{dr}(r\tilde{B}_r)_{r=a-}, \tag{17}$$

$$\Delta_+ = \frac{1}{\tilde{B}_a} \frac{d}{dr}(r\tilde{B}_r)_{r=a+}. \tag{18}$$

Additionally, the linearized induction equation can also be applied at $r = a_-$ with the result

$$\tilde{B}_a = (\mathbf{B}_0 \cdot \nabla)\tilde{\xi}_a. \tag{19}$$

With the constant current (and q) assumption for $r < a$, the eigenmode equation satisfies

$$[\frac{1}{r}\frac{d}{dr}(r\frac{d}{dr}) - \frac{1}{r^2}][\omega^2\mu_o\rho_o r\tilde{\xi}_r + (\mathbf{B}_o \cdot \nabla)r\tilde{B}_r] = 0. \tag{20}$$

Noting the regularity condition on axis, Eq. (15) becomes

$$\omega^2\mu_o\rho_o\tilde{\xi}_a = (\mathbf{B}_0 \cdot \nabla)\tilde{B}_a(\Delta_+ - 1) + iB_0\lambda_0\tilde{B}_a. \tag{21}$$

In order to complete the problem, a calculation of the quantity Δ_+ is required. This depends on the resistive wall properties in the $r > a$ region and will be discussed in detail in the following sections. For now, it is sufficient to treat this quantity as known and independent of z.

To this point, no restrictions on the z dependence of the eigenmode have been identified. From equations (19) and (21), an equation for the displacement at the plasma boundary is constructed

$$\omega^2\rho_o\mu_o\tilde{\xi}_a = (\mathbf{B}_0 \cdot \nabla)^2\tilde{\xi}_a(\Delta_+ - 1) + iB\lambda_o(\mathbf{B}_0 \cdot \nabla)\tilde{\xi}_a. \tag{22}$$

Using $\tilde{\xi}_a = \xi(z)e^{i\theta}$, Eq. (22) becomes a second order differential equation for $\xi(z)$ given by

$$\begin{aligned}\omega^2\frac{\rho_o\mu_o}{B_{z0}^2}\xi = (&\frac{d^2\xi}{dz^2} + 2i\frac{B_{\theta a}}{aB_{z0}}\frac{d\xi}{dz} - \frac{B_{\theta a}^2}{a^2B_{z0}^2}\xi)(\Delta_+ - 1) \\ &+\lambda_o(i\frac{d\xi}{dz} - \frac{B_{\theta a}}{aB_{z0}}\xi) = 0,\end{aligned} \tag{23}$$

where $B_{\theta a} = B_{\theta 0}(r = a)$. Looking for solutions of the form $\sim e^{ikz}$ uncovers two roots

$$k_{1,2} = -\frac{B_{\theta a}}{aB_{z0}} + \frac{\lambda_o}{2(1-\Delta_+)} \pm \sqrt{\frac{\lambda_o^2}{4(1-\Delta_+)^2} + \frac{\omega^2}{v_A^2(1-\Delta_+)}}, \tag{24}$$

where $v_A^2 = B_{z0}^2/\mu_o\rho_o$. The requirement of line tying specifies the boundary conditions $\tilde{B}_r(z=0) = \tilde{B}_r(z=L) = 0$. From Eq. (24), the solution for $\tilde{B}_r$ will be a linear combination of $e^{ik_1 z}$ and $e^{ik_2 z}$. The line tying boundary conditions can be satisfied by demanding the quantization condition

$$k_1 - k_2 = \frac{2n\pi}{L}, \tag{25}$$

where n is an integer. In this case, the magnetic perturbation takes the form

$$\tilde{B}_r = f(r)e^{i\theta + i(k_1+k_2)z/2} sin(\frac{n\pi z}{L}). \tag{26}$$

The quantization condition for line tying produces an eigenvalue equation for the growth rate

$$\frac{2n\pi}{L} = \sqrt{\frac{\lambda_o^2}{(1-\Delta_+)^2} + \frac{4\omega^2}{v_A^2(1-\Delta_+)}}, \tag{27}$$

or equivalently using the definition for q

$$n = \sqrt{\frac{4}{q_a^2(1-\Delta_+)^2} + \frac{4\omega^2\tau_A^2}{1-\Delta_+}}, \tag{28}$$

where $\tau_A = L/2\pi v_A$.

C. Resistive wall boundary conditions

In this section, the behavior of the magnetic perturbation in the regions outside the plasma boundary is described. In particular, two resistive walls are present at radial locations $r = b$ and $r = c$ ($a \leq b \leq c$). There are three distinct vacuum regions in general corresponding to the

region between the plasma and the first wall, the region between the two walls, and the region outside the second wall. The magnetic field satisfies $\mathbf{B} = \nabla\tilde{\phi}, \tilde{\phi} = e^{i\theta}\phi, \nabla^2\tilde{\phi} = 0$ in the vacuum regions. Using the high aspect ratio approximation, ϕ can be written as linear combinations of r and $1/r$ with coefficients that are arbitrary functions of z in the three distinct vacuum regions.

The coefficients are related by boundary conditions at both walls and at infinity. For the treatment of the resistive walls, a thin wall approximation is used ($\delta_b \ll b$, $\delta_c \ll c$ where δ_b and δ_c are the widths of the walls at $r = b$ and $r = c$, respectively). Two boundary conditions are given by continuity of the radial magnetic field at each wall. The effect of differential rotation is accounted for by treating the first wall at $r = b$ as stationary while the wall ar $r = c$ is rotating poloidally with speed V_c. The behavior of the radial magnetic field in each of the walls is governed by the linear induction equation

$$\frac{\partial\tilde{B}_r}{\partial t} + \mathbf{V}\cdot\nabla\tilde{B}_r = \frac{\eta_i}{\mu_o}\frac{1}{r}\nabla^2(r\tilde{B}_r), \tag{29}$$

with η_i denoting the resistivity of wall $i = (b, c)$. With the thin wall assumption, a relationship between the radial magnetic field and the eddy current flowing in the wall is derived by integrating across each wall.

$$\gamma\tau_b\tilde{B}_r|_{r=b} = b\frac{d\tilde{B}_r}{dr}|^{r=b+}_{r=b-}, \tag{30}$$

$$(\gamma + i\frac{V_c}{c})\tau_c\tilde{B}_r|_{r=c} = c\frac{d\tilde{B}_r}{dr}|^{r=c+}_{r=c-}, \tag{31}$$

where $\tau_b = \mu_o b \delta_b / \eta_b$, $\tau_c = c \delta_c \mu_o / \eta_c$ denotes the time constants for each wall and γ is the growth rate. For convenience, we define the quantities

$$\Delta_b = \frac{\gamma \tau_b}{2}, \tag{32}$$

$$\Delta_c = \frac{\gamma \tau_c}{2} + i \frac{R_c}{2}, \tag{33}$$

where $R_c = V_c \tau_c / c = V_c \delta_c \mu_o / \eta_c$ is the Reynolds number of the rotating wall.

The quantity of interest relative to stability is Δ_+ defined by Eq. (18). Using the boundary conditions describe above, this is easily derived and given by

$$\Delta_+ = \frac{-1 - \Delta_b[1 + (\frac{a}{b})^2] - \Delta_c[1 + (\frac{a}{c})^2] - \Delta_b \Delta_c [1 + (\frac{a}{b})^2][1 - (\frac{b}{c})^2]}{1 + \Delta_b[1 - (\frac{a}{b})^2] + \Delta_c[1 - (\frac{a}{c})^2] + \Delta_b \Delta_c [1 - (\frac{a}{b})^2][1 - (\frac{b}{c})^2]}. \tag{34}$$

Throughout this calculation, the boundary conditions at $z = 0, L$ are still satisfied. This is valid as long as the wall times of the resistive walls are short relative to the timescales of the end wall plates. This is easily satisfied in the configuration described in Ref. [19].

D. Dispersion relation

Having determined Δ_+, an equation for the growth rate is derived. The $n = 1$ case is treated in the following since it is the most unstable mode. Before looking specifically at the resistive wall mode dispersion relation, we can identify the ideal kink stability conditions. Namely, the no-wall dispersion relation is identified by setting $\Delta_b = \Delta_c = 0$ ($\Delta_+ = -1$), and one finds

$$\omega^2 \tau_A^2 = \frac{1}{2}(1 - \frac{1}{q_a^2}). \tag{35}$$

The instability condition corresponds to the familiar Kruskal-Shafranov criteria; $q_a < 1$ indicates instability [20, 21]. For a perfectly conducting wall at $r = b$, $\Delta_b \to \infty$. In this limit, $1 - \Delta_+ = 2/[1 - (a/b)^2]$ and the dispersion relation becomes

$$\omega^2 \tau_A^2 = \frac{1}{2[1 - (\frac{a}{b})^2]} \{1 - \frac{[1 - (\frac{a}{b})^2]^2}{q_a^2}\}. \tag{36}$$

The instability condition is given by [8]

$$q_a - 1 + (\frac{a}{b})^2 < 0, \tag{37}$$

For a close fitting conducting wall $b \to a$, the external kink is stabilized.

The case of interest for resistive wall instability is when the plasma is unstable with the wall at infinity and stable in the presence of a perfectly conducting wall. In this limit, we seek solutions which grow with the characteristic time for a magnetic signal to soak through the resistive wall. Since the wall times are usually much longer than the Alfven time, the kinetic energy in the mode is negligible and the dispersion relation is simply $1 - \Delta_+ = 2/q_a$. For the case of a single wall at $r = b$ ($\Delta_c = 0$) the growth rate is

$$\gamma = \frac{2}{\tau_b} \frac{1 - q_a}{q_a - 1 + (\frac{a}{b})^2}. \tag{38}$$

For $1 > q_a > 1 - (\frac{a}{b})^2$, the resistive wall is unstable. For convenience, the following notation is introduced to indicate the strength of the instability for the cases of no-wall, a perfectly conducting wall at $r = b$ and a perfectly conducting wall ar $r = c$, respectively

$$X_\infty = 1 - \frac{1}{q_a}, \tag{39}$$

$$X_b = 1 - \frac{1 - (\frac{a}{b})^2}{q_a}, \tag{40}$$

$$X_c = 1 - \frac{1 - (\frac{a}{c})^2}{q_a}. \tag{41}$$

With this notation, $\gamma\tau_b/2 = -X_\infty/X_b$; X_i indicates the strength of the ideal MHD drive for each configuration.

Next we deal with the more general case of two resistive walls. Using the notation of Eqs. (39)-(41), the dispersion relation becomes

$$X_\infty + \Delta_b X_b + \Delta_c X_c + \Delta_b \Delta_c X_b \epsilon = 0 \tag{42}$$

where

$$\epsilon = 1 - (\frac{b}{c})^2 = \frac{X_b - X_c}{X_b - X_\infty}. \tag{43}$$

If $\epsilon \to 0$, the two walls lie on top of each other and effectively become a single wall. The general solution has two roots when $\epsilon \neq 0$.

In the limit that the walls are stationary, the dispersion relation is a quadratic equation for the growth rate and given by the two roots

$$\gamma = -\frac{1}{\epsilon}[\frac{1}{\tau_c} + \frac{X_c}{\tau_b X_b}] \pm \frac{1}{\epsilon}\sqrt{[\frac{1}{\tau_c} + \frac{X_c}{\tau_b X_b}]^2 - \frac{4X_\infty \epsilon}{X_b \tau_b \tau_c}}. \tag{44}$$

As in the single wall case, for $X_\infty < 0$, there is always one root which is destabilized. In the small ϵ limit, the decay rate of the second stable root is nearly independent of the plasma properties and essentially describes the the L/R time of the double wall configuration.

Inclusion of the rotation in the RWM dispersion relation yields complex eigenvalues. Assuming solutions of the form $e^{-i\omega t}$, the disperion relationship

is given by

$$\omega^2 X_b + \frac{i\omega}{\epsilon}(\frac{2X_b}{\tau_c} + \frac{2X_c}{\tau_b}) - \omega\frac{R_c X_b}{\tau_c} - \frac{i2R_c X_c}{\epsilon\tau_b\tau_c} - \frac{4X_\infty}{\epsilon\tau_b\tau_c} = 0. \tag{45}$$

The two roots of this equation have both real and imaginary parts:

$$Re(\omega) = \frac{R_c}{2\tau_c} \mp \sqrt{\sqrt{A^2+B^2} - A} \tag{46}$$

$$\gamma = -\frac{1}{\epsilon}(\frac{1}{\tau_c} + \frac{X_c}{X_b\tau_b}) \pm \sqrt{\sqrt{A^2+B^2} + A}, \tag{47}$$

where

$$A = -\frac{2X_\infty}{\epsilon X_b\tau_b\tau_c} + \frac{1}{2\epsilon^2}(\frac{1}{\tau_c} + \frac{X_c}{X_b\tau_b})^2 - \frac{R_c^2}{8\tau_c^2} \tag{48}$$

$$B = \frac{R_c}{2\epsilon}(\frac{1}{\tau_c^2} - \frac{X_c}{X_b\tau_b\tau_c}). \tag{49}$$

The growth rate and frequency as functions of R_c is plotted in Figure 1 for $q_a = 0.8$. For low rotation, the linear growth and damping rates of Eq. (44) are recovered. As R_c increases, the growth rate decreases and becomes stabilized at large enough rotation. For large R_c, the growth rates approach the asymptotic limits, $\gamma \approx -2X_c/(\epsilon X_b\tau_b), -2/(\epsilon\tau_c)$ with real frequencies $\omega \approx 0, R_c\tau_c = V_c/c$. Additionally, as shown in Figure 2, for a fixed rotation rate, the growth decays as q_a rises.

For sufficiently high R_c, the growth rate changes sign. The critical value of R_c necessary for stabilization can be found from Eq. (47) and is given by

$$R_{c,crit}^2 = 4\frac{-X_\infty X_b + X_\infty^2}{X_c(X_b - X_c)}[1 + \frac{\tau_c X_c}{\tau_b X_b}]^2. \tag{50}$$

This solution is plotted in Figure 3 and shows that the critical R_c rises as q_a drops below unity.

The critical magnetic Reynolds number becomes large in two limits, when $X_c \to 0$ and when $X_c \to X_b$. In the $X_c = 0$ limit, $r = c$ corresponds to the critical radius for marginal kink stability; the stabilization process requires that both walls are inside the critical radius. The second limit corresponds to the case where the radial separation between the two walls shrinks to zero. Stabilization requires a finite inductance in the exterior wall configuration (as measured by the parameter ϵ). The presence of ϵ allows for a phase shift between the two walls which, in the presence of rotation, couples the stable RWM root of Eq. (44) to the destabilizing root. In Figure 4, a plot of critical rotation rate versus second wall location is shown for varius values of q_a.

There is a critical value of X_c that minimizes the required R_c. This is given by

$$X_c = X_b \frac{1}{2 + (\tau_c/\tau_b)}. \tag{51}$$

Evaluating the critical Reynolds number at the miminum value of X_c, we obtain a minimum critical rotation rate

$$R_{c,crit,min} = 8\sqrt{\frac{X + X^2}{2}}\sqrt{\frac{1 + \tau_c/\tau_b}{2}} \tag{52}$$

where $X = -X_\infty/X_b$. The critical condition on X_c can be translated into an optimal location of the wall position c. Using the approximation $kc << 1$, this is given by

$$(\frac{a}{c})^2 = 1 - q_a[1 - \frac{X_b}{2 + (\tau_c/\tau_b)}] \tag{53}$$

which becomes $(a/c)^2 = 1 - 2q_a/3$ in the limit that $b = a$ ($X_b = 1$) and $\tau_c = \tau_b$. As the plasma becomes more unstable (X becomes larger), the

optimal wall radius shrinks.

For a fixed value of $(a/c)^2$, the critical Reynolds number rises with $-X_\infty$. Using $b = a$ and $\tau_c = \tau_b$, Eq. (50) can be rewritten

$$R^2_{c,crit} = \frac{4(X + X^2)}{[(\frac{a}{c})^2 - \frac{X}{1+X}][1 - (\frac{a}{c})^2]}[\frac{1 - X}{1 + X} + (\frac{a}{c})^2]^2. \tag{54}$$

Using the expression for X in Eq. (39), the critical rotation frequency can be written

$$R^2_{c,crit} = \frac{4}{q_a^2}\frac{1 - q_a}{[1 - (\frac{a}{c})^2][(\frac{a}{c})^2 - 1 + q_a]}[2q_a - 1 + (\frac{a}{c})^2]^2. \tag{55}$$

III. RESISTIVE WALL STABILITY IN THE PERIODIC CYLINDER

Analysis of resistive wall instability in a periodic cylinder differs from the line tied case in the treatment of the z dependence of the perturbation. For the periodic cylinder, a Fourier representation for the magnetic perturbation is appropriate, $\tilde{B}_r \sim e^{im\theta - in\zeta}$ where m and n are integers and the effective toroidal angle can be defined $\zeta = 2\pi z/L$.

As in the treatment given in Section II, it is usually assumed that the timescale of the instability is slow compared to ideal MHD times. In this case, the marginal ideal MHD equations are sufficient to describe the plasma response and the strength of the instability is measured by the potential energy, δW, corresponding to the cases with perfectly conducting walls [22].

For a constant current profile, the marginal stability is well-known [23] and easily derived from Eq. (22) by setting $\omega^2 = 0$ and having $\mathbf{B}_o \cdot \nabla = (m - nq)B_{\theta 0}/r$. In this case, the marginal stability condition is given simply by

$$1 - \Delta + = \frac{2}{m - nq_a}, \tag{56}$$

where $\Delta+$ is given by Eq. (38) in general. In the absence of any conducting walls, $\Delta+ = -1$, and marginal stability is given by $1 - 1/(m - nq_a) = 0$. Equivilantly, the ideal MHD potential energy is given by

$$\frac{\delta W}{\pi a^2 L} = \frac{2|\tilde{B}_a|^2}{\mu_o}(1 - \frac{1}{m - nq_a}). \tag{57}$$

Similarly, in the limit of a perfectly conducting wall at $r = b$, the marginal ideal stability condition becomes

$$1 - \frac{1 - (\frac{a}{b})^{2m}}{m - nq_a} = 0. \tag{58}$$

In analogy with Eqs. (39)-(41), one can indicate the strength of the instability for the cases of no-wall, a perfectly conducting wall at $r = b$ and a perfectly conducting wall at $r = c$, respectively, by

$$X_\infty^{pc} = 1 - \frac{1}{m - nq_a}, \tag{59}$$

$$X_b^{pc} = 1 - \frac{1 - (\frac{a}{b})^{2m}}{m - nq_a}, \tag{60}$$

$$X_c^{pc} = 1 - \frac{1 - (\frac{a}{c})^{2m}}{m - nq_a}, \tag{61}$$

where the superscript pc corresponds to periodic cylinder. For the general case of the two resistive walls, one of which rotates, the dispersion relation

for the periodic cylinder case takes on precisely the same form as for the line tied case

$$X_{\infty}^{pc} + \Delta_b X_b^{pc} + \Delta_c X_c^{pc} + \Delta_b \Delta_c X_b^{pc} \epsilon = 0, \tag{62}$$

where Δ_b, Δ_c, and ϵ are defined in Eqs. (32), (33) and (43), respectively. The major difference is in the identification of the MHD potential energy. However, all of the formulae dervied in Section II.D following Eq. (42) are equally valid for the periodic cylinder case.

Unlike the line tied case, the plasma becomes highly unstable as a low order rational appears just outside the plasma-vacuum interface. For the line tied case, rational surfaces do not play a role as the eigenfunction is given by a standing wave. To demonstrate this difference, compare the minimum required rotation rate in the case where the second wall location is optimizally chosen. This rotation rate is denoted $R_{c,crit,min}$ and given by Eq. (52). For the special limit $a = b$, $\tau_b = \tau_c$, the minimum critical rotation rate for the line tied case is given by

$$R_{c,crit,min} = 4\frac{\sqrt{2(1-q_a)}}{q_a}. \tag{63}$$

The corresponding case for the periodic cylinder is given by

$$R_{c,crit,min}^{pc} = 4\frac{\sqrt{2(1-m+nq_a)}}{m-nq_a}. \tag{64}$$

Consequently, the Gimblett double wall configuration can stabilize RWMs so long as q_a is not too far from a rational value, but the requirements for rotational stabilization become prohibitive as q_a drops just below a rational

value ($m - nq_a \ll 1$).

IV. DISCUSSION

In this work, a dispersion relation is derived for the resistive wall stability of a high aspect ratio screw pinch equilibrium in the presence of perfectly conducting end walls. Additionally, the effect of two differentially rotating, radially separated resistive walls is included in the analysis. The calculations demonstrate that as in the periodic cylinder case, differential rotation of two radially separated resistive walls can be used to stabilize the resistive wall modes.

As a specific example we treat the case of a zero plasma pressure, constant current profile equilibrium with $B_\theta \ll B_z$. In the presence of perfectly conducting end walls, ideal kink stability in the no radial wall limit is governed by the simple instability criteria $q_a < 1$ for $m = 1$ modes. When a perfectly conducting wall is placed at $r = b$, the instability criterion is given by $q_a < 1 - (a/b)^2$. Hence, there is a regime where the plasma is unstable without a conducting wall and stable with a perfectly conducting wall at $r = b$. It is in this regime where resistive wall modes become unstable.

Following the suggestion of Gimblett[1], the presence of a second rotating wall can stabilize the resistive wall mode if the second wall is sufficiently close to stabilize the ideal and kink. As in the periodic cylinder case, there exist a critical wall location for the second wall that minimizes the necessary rotation for stabilization.

A comparison can be directly made between the line tied case and the case of a periodic cylinder. With the use of the large aspect ratio approximation, the vacuum and resistive wall solutions are identical for the two cases. The differences lie in the describing the plasma free energy through the parameters X_i. The relevant measure in the periodic cylinder case, where the magnetic perturbation is given by a Fourier mode $\tilde{\mathbf{B}} \sim e^{im\theta - in\zeta}$ is given by the quantity $X^{pc}_{\infty} = 1 - 1/(m - nq_a)$. This shows the well known result that external kink modes are easily destabilized when the rational surface of the Fourier mode lies just outside of the plasma-vacuum interface. In the case of a small value of $m - nq_a$, it is very difficult to stabilize the RWM with rotating walls. In the presence of line tied boundary conditions, there is no single "rational" surface and the stability conditions are simply related to the total current in the device and the presence of the walls.

Acknowledgments

The authors would like to acknowledge fruitful discussions with Cary Forest, Carl Sovinec, John Sarff, Gennedy Fiksel, Ellen Zweibel and Stewart Prager. This work is supported by the U. S. Department of Energy under contracts DE-FG02-86ER53218 and DE-FG02-85ER53212.

References

[1] C. G. Gimblett, Plasma Phys. Controlled Fusion **31**, 2183 (1989).

[2] C. C. Hegna and C. B. Forest, "Stabilization of Resistive Wall Modes with Rotating Walls," UW-CPTC Report 00-03 (May, 2000).

[3] J. P. Friedberg and R. Betti, Phys. Plasmas **8**, 1 (2001).

[4] J. B. Taylor, J. W. Connor, C. G. Gimblett, H. R. Wilson, and R. J. Hastie, Phys. Plasmas **8**, 4062 (2001).

[5] M. V. Umansky, R. Betti and J. P. Friedberg, Phys. Plasmas **8**, 4427 (2001).

[6] G. Einaudi and G. Van Hoven, Phys. Fluids **24**, 1092 (1981).

[7] M. Velli, G. Einaudi, and A. W. Hood, Astrophys. J. **350**, 419 (1990); Astrophys. J. **350**, 426 (1990).

[8] D. D. Ryutov, R. H. Cohen, and L. D. Pearlstein, Bull Am. Phys. Soc. **48**, 167 (2003).

[9] A. Bondeson and D. J. Ward, Phys. Rev. Lett. **72**, 2709 (1994).

[10] B. Alper, M. K. Bevir, H. A. B. Bodin et al, Plasma Phys. Controlled Fusion **31**, 205 (1989).

[11] A. M. Garofalo, A. D. Turnbull, M. E. Austin et al, Phys. Rev. Lett. **82**, 3811 (1999).

[12] A. M. Garafalo, T. H. Jensen, L. C. Johnson et al, Phys. Plasmas **9**, 1997 (2002).

[13] C. M. Bishop, Plasma Phys. Controlled Fusion **31**, 1179 (1989).

[14] T. H. Ivers, E. Eisner, A. Garofalo et al, Phys. Plasmas **3**, 1926 (1996).

[15] A. M. Garofalo, T. H. Jensen, and E. J. Strait, Phys. Plasmas **9**, 4573 (2002).

[16] S. I. Krasheninnikov, L. E. Zakharov, and G. V. Pereverzev, Phys. Plasmas **10**, 1678 (2003).

[17] J. M. Finn, Phys. Plasmas **2**, 3782 (1995).

[18] C. G. Gimblett and R. J. Hastie, Phys. Plasmas **7**, 258 (2000); Phys. Plasmas **11**, 1019 (2004).

[19] C. B. Forest, C. C. Hegna, G. Fiksel, and J. S. Sarff, Bull. Am. Phys. Soc. **45**, 330 (2000).

[20] M. D. Kruskal and M. Schwarzschild, Proc. R. Soc. London, Ser. A, **223**, 348 (1954).

[21] V. D. Shafranov, At. Energy **5**, 38 (1956).

[22] J. P. Friedberg, "Ideal Magnetohydrodynamics," Plenum Press, New York, New York, pp. 307-314 (1987).

[23] V. D. Shafranov, Sov. Phys. Tech. **15**, 175 (1970).

Figure Captions

1. The growth rates (solid line) and real frequencies (dotted lines) corresponding to parameters of the UW rotating wall experiment as calculated from Eqs. (46) and (47). The parameters used are $a = 9.5cm, b = 10.2cm, c = 12.6cm, \tau_b = 11.6ms, \tau_c = 14.5ms$. As R_c increases, the growth rate of the unstable mode decreases and becomes stabilized are large enough rotation. For large R_c, the asymptotic limits, $\gamma \approx -2X_c/(\epsilon X_b \tau_b), -2/(\epsilon\tau_c)$, $\omega \approx 0, mV_c/c$ are approached.

2. The growth rate of the unstable mode as a function of q_a for different values of R_c for the same parameters as Fig. 1. For no rotation, the instability onsets with $q_a < 1$. For higher values of R_c, stable operation can be achieved at lower q_a. The solid, dotted, dashed and dash-dotted curves correspond to $R_c = 0, 3, 6, 9$, respectively.

3. The critical rotation rate for stabilization vs. q_a as calculated from Eq. (50). The critical rotation rate rises monotonically as q_a drops below unity.

4. The critical R_c as defined by Eq. (50) versus the location of the second wall as measured by the ratio c/b using $b = a$ and $c \ll L$. The solid, dotted, dashed, and dash-dotted lines correspond to $q_a = 0.5, 0.6, 0.7, 0.8$, respectively. The lower q_a, the more unstable the plasma with the wall at infinity.

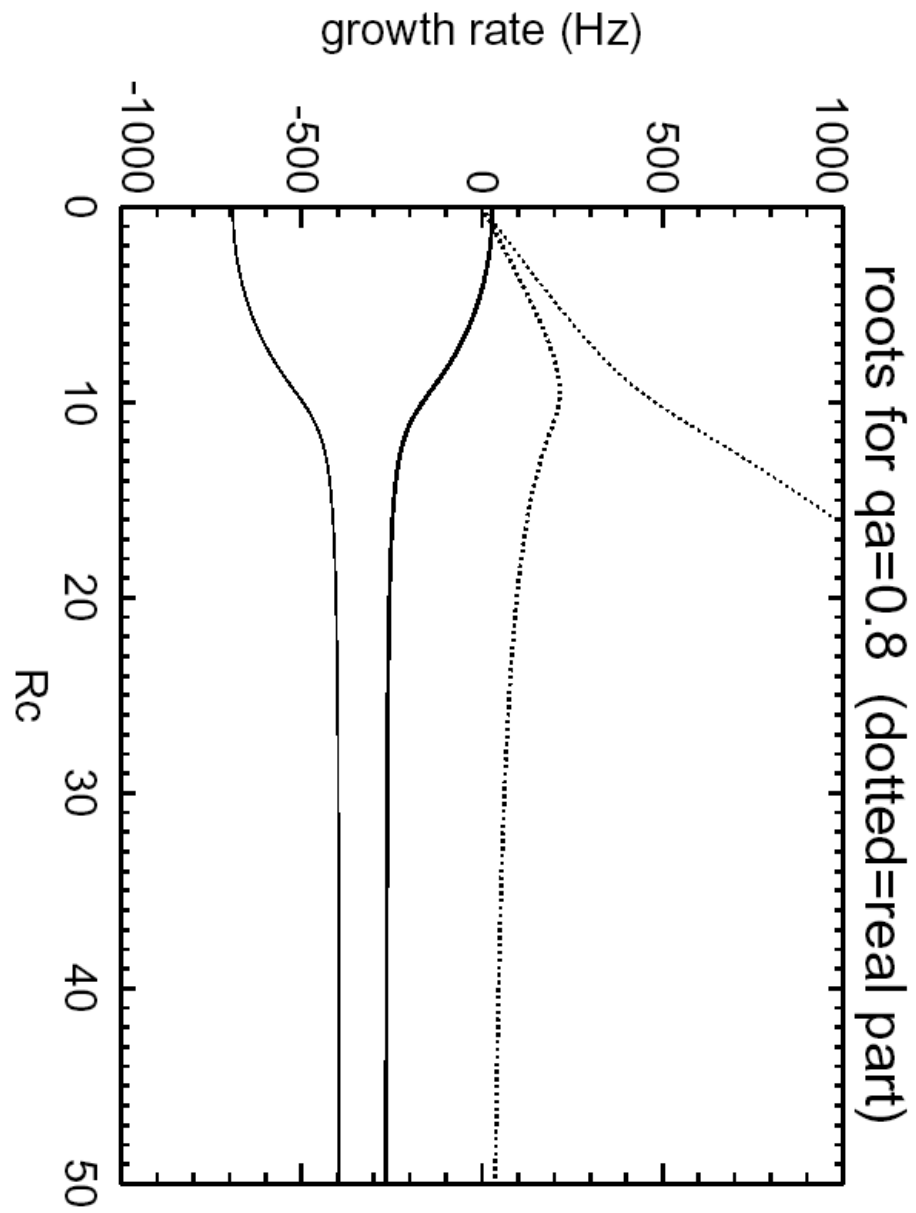
growth rate (Hz)
-1000
-500
0
500
1000
roots for qa=0.8 (dotted=real part)
0
10
20
30
40
50
Rc

Figure 1

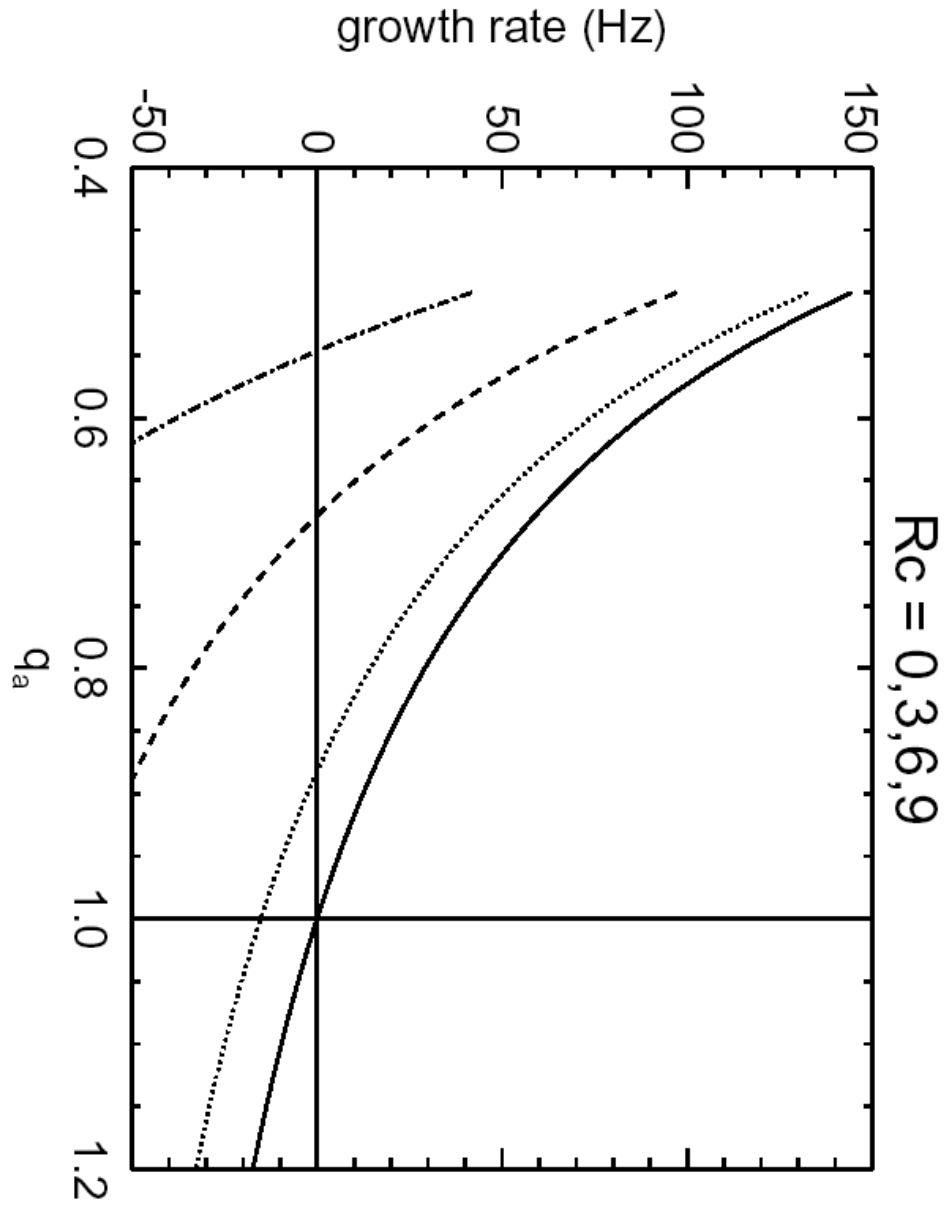

Figure 2

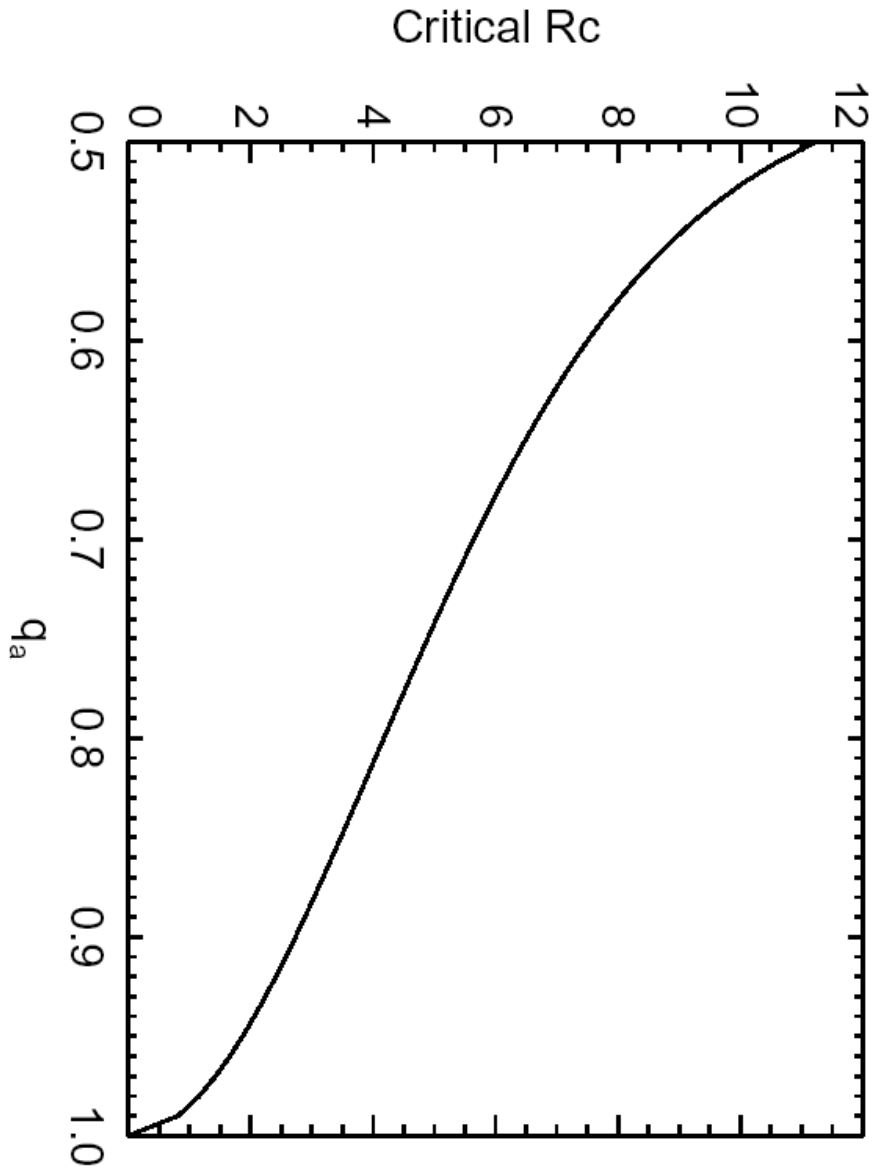

Figure 3

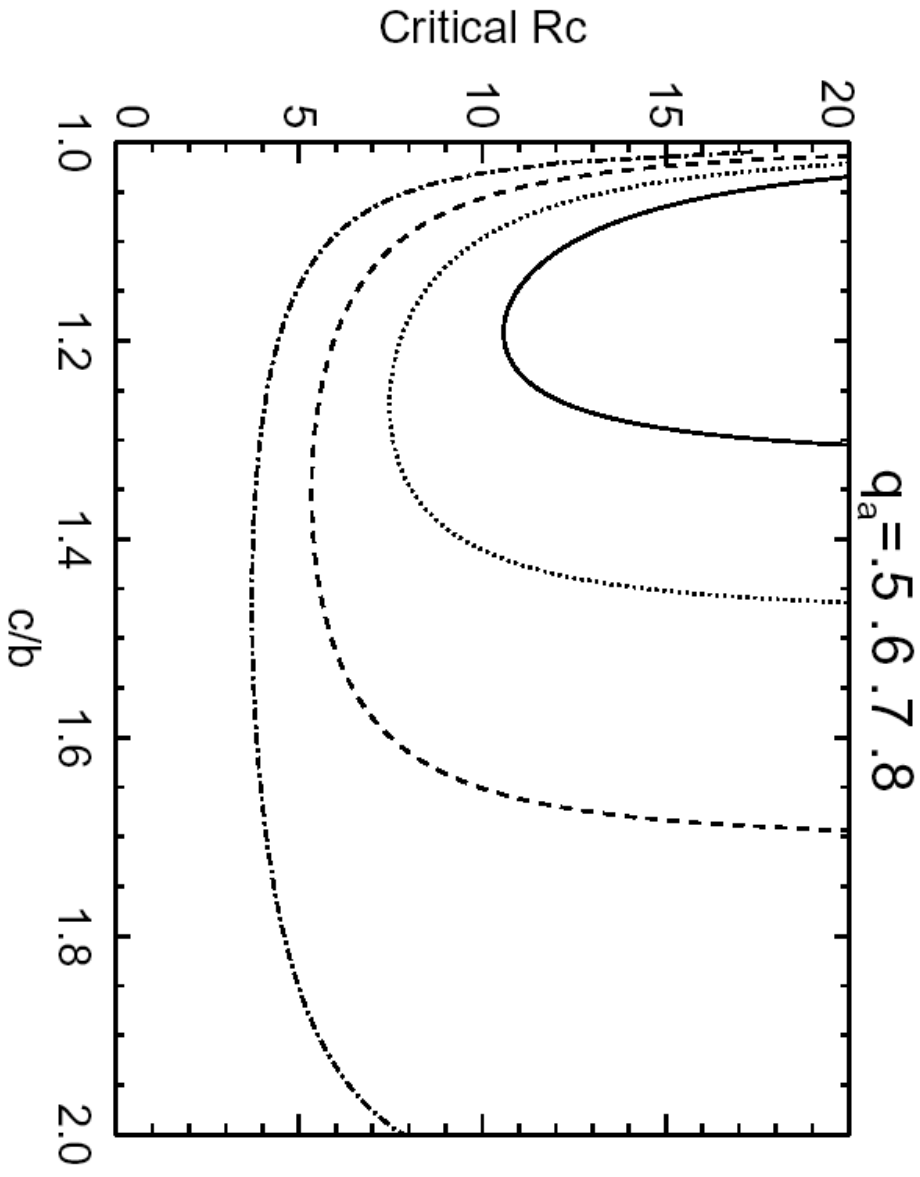

Figure 4